Adaptive Multiscale Moment Method (AMMM) for Analysis of Scattering from Perfectly Conducting Plates

Chaowei Su and T. K. Sarkar, *Fellow, IEEE*

***Abstract*—Adaptive multiscale moment method (AMMM) is presented for the analysis of scattering from a thin perfectly conducting plate. This algorithm employs the conventional moment method and a special matrix transformation, which is derived from the tensor products of the two one-dimensional (1-D) multiscale triangular basis functions that are used for expansion and testing functions in the conventional moment method. The special feature of these new basis functions introduced through this transformation is that they are orthogonal at the same scale except at the initial scale and not between scales. From one scale to another scale, the initial estimate for the solution can be predicted using this multiscale technique. Hence, the compression is applied directly to the solution and the size of the linear equations to be solved is reduced, thereby improving the efficiency of the conventional moment method. The basic difference between this methodology and the other techniques that have been presented so far is that we apply the compression not to the impedance matrix, but to the solution itself directly using an iterative solution methodology. The extrapolated results at the higher scale thus provide a good initial guess for the iterative method. Typically, when the number of unknowns exceeds a few thousand unknowns, the matrix solution time exceeds generally the matrix fill time. Hence, the goal of this method is directed in solving electrically larger problems, where the matrix solution time is of concern. Two numerical results are presented, which demonstrate that the AMMM is a useful method to analyze scattering from perfectly conducting plates.**

***Index Terms*—Electromagnetic scattering, method of moments.**

I. Introduction

THE moment method is one of the most popular numerical techniques to analyze the scattering and radiation from complex structures, which has been in use over the past 30 years [1], [2]. However, when the size of scatterers or radiators is electrically large and even resonant, the moment method becomes computationally too expensive (too much memory and CPU time) to analyze them.

In order to overcome the difficulty of the moment method, many types of hybrid approaches that are based on high-frequency and low-frequency techniques have been proposed. A review of these hybrid techniques can been found in [3]–[5]. Although these hybrid techniques can deal with scattering and radiating complex objects, for the solution of scattering from electrically large complex objects it is a big computational challenge. Recently, many researchers have tried to solve directly these large computationally intensive problems by the combination of the conventional method of moments (MoM) and other new techniques. In these new techniques there are the impedance matrix localization method (IML) [6]–[9]), the fast multipole method (FMM) [10]–[12], the complex multipole beam approach (CMBA) [13], the matrix decomposition algorithm (MDA) [14], and its multilevel cousin: a multilevel matrix decomposition algorithm (MLMDA) [15], [16], wavelet method [17]–[21], [36], etc. A detailed discussion of these fast solution methods for efficiently solving large electromagnetic problems is provided in [22].

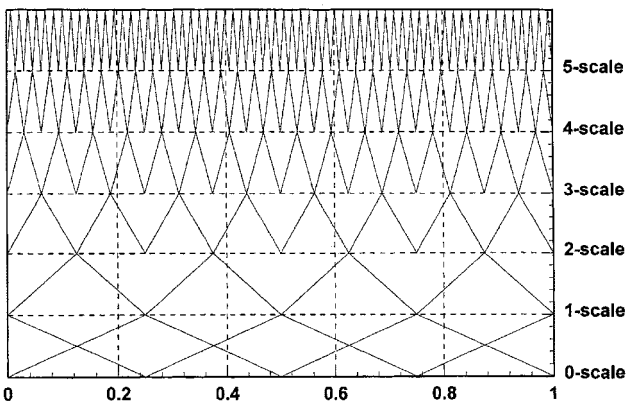

Fig. 1. The multiscale basis functions $\Psi_{\Pi}^{4,5}(x)$ on the domain [0,1].

Another method is the adaptive multiscale moment method (AMMM) proposed by the authors [23]–[27], which is a hybrid technique combining the multigrid method with the compression methodology. The distinction of this method over other is that the compression is used directly on the solution itself, even though it is unknown.

As we know, the multilevel or the multigrid technique has been widely used in solving the differential equations and integral equations [28]–[32]. Kalbasi and Demarest [33], [34] applied the multilevel concepts to solve the integral equation by the moment method on different levels, which has been called the multilevel moment method (MMM). MMM can predict reasonably the initial solution on the fine grid from the known solution on the coarse grid so that it can reduce the number of iteration required to generate the solution at that scale.

Mathematically, the compression methodology tries to approximate the original function with a little loss of accuracy

Manuscript received December 15, 1998; revised November 19, 1999.

C. Su is with the Department of Applied Mathematics, Northwestern Polytechnical University, Xian, Shaanxi, China.

T. K. Sarkar is with the Department of Electrical and Computer Engineering, Syracuse University, Syracuse, NY 13244 USA.

Publisher Item Identifier S 0018-926X(00)05795-1.

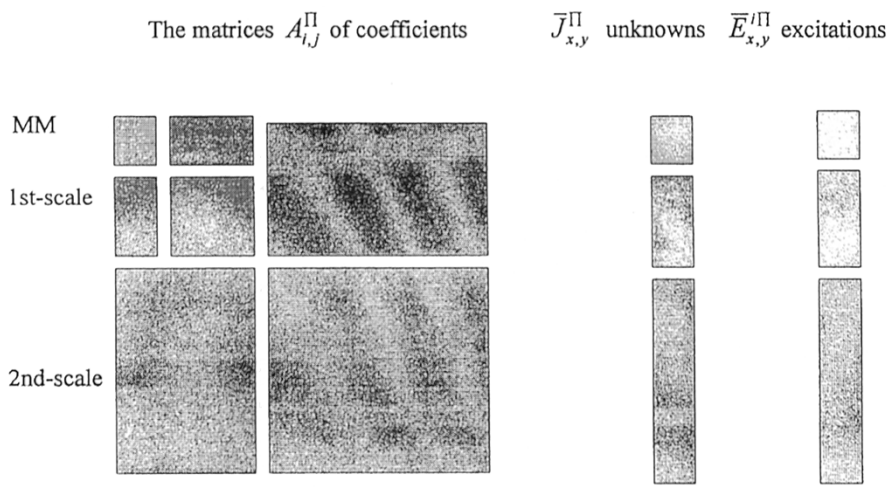

Fig. 2. The illustration of coefficient matrices, the right arrays and the unknowns.

by using a few basis functions introduced through the tensor product. The wavelet method is an important digital compression method to compress the data. Hence, many researchers [17]–[21], [36] chose the wavelet basis function or wavelet-like basis function in the moment method because the impedance matrix will be sparse. They used the wavelet method to compress the impedance matrix and not the solution. Hence, the scaling function in a wavelet method is neglected and so is the relationship between the scaling function and the solution.

In AMMM, the authors proposed a special kind of multiscale basis functions on a bounded region, which is similar to a wavelet-like basis functions. For one-dimensional case (1-D), the multiscale basis functions possess three important properties. First, they are equivalent to the triangular basis functions on the bounded interval. Second, these new basis functions are orthogonal among themselves on the new scale and are zero at the nodes of the previous scale. However, they are not orthogonal between the scales. Third, if the unknown solution has a linear behavior, then the number of basis functions will not increase at the higher scale when the scale is increased. For the two-dimensional (2-D) case [27], the basis functions constructed by the tensor product of two multiscale basis functions possess three important properties. The solution on different scales corresponds to the solution at the different level grids in the multigrid method. Therefore, AMMM possesses three characteristics.

1) The moment matrix on the multiscale basis can be computed directly from the original moment matrix utilizing the conventionally used triangular basis through a basis transformation matrix. Hence, conventional codes using triangular patches can be used to evaluate the MoM matrix.
2) When the scale is increased, the initial guess for the solution utilized in an iterative solver at the new scale can be obtained from the initial guess of the multigrid method at the new scale.
3) The size of the linear equations are reduced through thresholding the small coefficients of the unknown solution by *a priori* threshold.

Our motivation in the present paper is to apply a 2-D AMMM to analyze scattering by thin perfectly conducting plates. Section II introduces the 2-D multiscale basis according to the tensor product of the 1-D multiscale triangular basis. A 2-D function can be approached approximately by the linear combination of 2-D multiscale basis. Section III directly discretizes the EFIE based on the tensor product of the triangular basis by Galerkin method and presents the formula of the linear equations for the 2-D multiscale basis. Then the 2-D AMMM is presented to solve the linear equations. Our goal is to reduce the matrix solution time for large problems. Section IV presents two numerical examples for analyzing scattering from perfectly conducting square plates.

II. 2-D Multiscale Basis Functions and Function Approximation

The multiscale basis functions in AMMM [23], [24] are based on the use of a uniform grid and the conventional triangular basis functions. They can be obtained from the usual triangular basis by the use of a full-rank matrix transformation; that is

$$\Psi_{\Pi}^{N,V}(x) = T(N, V)\Phi_{\Delta}^{1+2^V N}(x) \tag{1}$$

where $\Phi_{\Delta}^{1+2^V N}(x) = (\phi_1(x), \cdots, \phi_{1+2^V N}(x))^T$ is the uniform triangular basis. $\Psi_{\Pi}^{N,V}(x) = (\psi_1(x), \cdots, \psi_{1+2^V N}(x))^T$ is the multiscale basis functions. The superscript T denotes the transpose of a matrix. N is the number of the initial division of the interval. V is the number of the largest scale and the interval is divided into $1 + 2^V N$ points. $T(N, V)$ is a full-rank matrix. Fig. 1 shows all of the multiscale basis functions $\Psi_{\Pi}^{4,5}(x)$ on [0, 1].

For the 2-D case, the basis functions can be constructed by a tensor product. Suppose the multiscale basis function and the triangular basis function for the x-directed components of the currents on a structure be $\Psi_{\Pi}^{N,V}(x) = (\psi_1(x), \cdots, \psi_{1+2^V N}(x))^T$, $\Phi_{\Delta}^{1+2^V N}(x) = (\phi_1(x), \cdots, \phi_{1+2^V N}(x))^T$, respectively. The multiscale basis function and the triangular basis function for the y-directed component of the solution are $\Psi_{\Pi}^{M,V}(y) = (\psi_1(y), \cdots, \psi_{1+2^V M}(y))^T$,

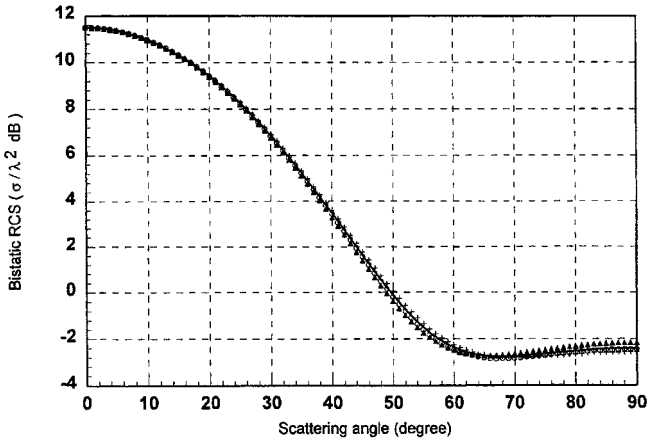

Fig. 3. The bistatic RCS of a 1.1 square plates by a normally incident plane wave versus the scattering angle on $\phi = 0^\circ$ plane. The circle, triangle, and cross signals denote the results for the threshold $\varepsilon = 0.01,\ 0.05,\ 0.1$. The soldi line denotes the result of the conventional moment method.

$\Phi_\Delta^{1+2^V M}(y) = (\phi_1(y), \cdots, \phi_{1+2^V M}(y))^T$, respectively. The basis functions in 2-D's can be written in the form of a tensor product

$$\Phi_\Delta^{1+2^V N}(x) \otimes \Phi_\Delta^{1+2^V M}(y) = \begin{pmatrix} \phi_1(x) \\ \vdots \\ \phi_{1+2^V N}(x) \end{pmatrix} (\phi_1(y) \cdots \phi_{1+2^V M}(y)),$$

for the triangular form

$$\Psi_\Pi^{N,V}(x) \otimes \Psi_\Pi^{M,V}(y) = \begin{pmatrix} \psi_1(x) \\ \vdots \\ \psi_{1+2^V N}(x) \end{pmatrix} (\psi_1(y) \cdots \psi_{1+2^V M}(y)),$$

for the multiscale form.

The relation between the multiscale basis and the triangular basis is given by

$$\begin{aligned} &\Psi_\Pi^{N,V}(x) \otimes \Psi_\Pi^{M,V}(y) \\ &\quad = T(N, V) \begin{pmatrix} \phi_1(x) \\ \vdots \\ \phi_{1+2^V N}(x) \end{pmatrix} (\phi_1(y) \cdots \phi_{1+2^V M}(y)) \\ &\qquad \cdot T'(M, V) \\ &\Psi_\Pi^{N,V}(x) \otimes \Psi_\Pi^{M,V}(y) \\ &\quad = T(N, V) \Phi_\Delta^{1+2^V N}(x) \otimes \Phi_\Delta^{1+2^V M}(y) T'(M, V). \end{aligned} \tag{2}$$

Now, we consider the approximation of a function $f(x, y)$ using these two kinds of basis. The function $f(x, y)$ can be approximated by these basis functions in the following form:

$$\begin{aligned} f(x, y) &= \sum_{i,j} f_{i,j}^\Delta \phi_i(x) \phi_j(y) \\ &= \left(\Phi_\Delta^{1+2^V N}(x)\right)' F^\Delta \Phi_\Delta^{1+2^V M}(y) \\ &= \sum_{i,j} f_{i,j}^\Pi \psi_j(y) \\ &= \left(\Psi_\Pi^{N,V}(x)\right)' F^\Pi \Psi_\Pi^{M,V}(y). \end{aligned} \tag{3}$$

F^Π and F^Δ have the following relationship:

$$F^\Pi = T'(N, V) F^\Delta T(M, V) \tag{4}$$

where

$$\begin{aligned} F^\Delta &= \begin{pmatrix} f(x_1, y_1) & \cdots & f(x_1, y_{1+2^V M}) \\ \vdots & \ddots & \vdots \\ f(x_{1+2^V N}, y_1) & \cdots & f(x_{1+2^V N}, y_{1+2^V M}) \end{pmatrix} \\ &= \begin{pmatrix} f_{1,1} & \cdots & f_{1,1+2^V M} \\ \vdots & \ddots & \vdots \\ f_{1+2^V N,1} & \cdots & f_{1+2^V N,1+2^V M} \end{pmatrix} \\ F^\Pi &= \begin{pmatrix} f_{1,1}^\Pi & \cdots & f_{1,1+2^V M}^\Pi \\ \vdots & \ddots & \vdots \\ f_{1+2^V N,1}^\Pi & \cdots & f_{1+2^V N,1+2^V M}^\Pi \end{pmatrix}. \end{aligned}$$

The geometrical means of the coefficients F^Π, F^Δ has been described in [27]. After filtering out some of the relatively small elements in F^Π through a threshold ε, we can obtain the new modified matrix

$$F^C = \begin{pmatrix} f_{1,1}^C & \cdots & f_{1,1+2^V N}^C \\ \vdots & \ddots & \vdots \\ f_{1+2^V N,1}^C & \cdots & f_{1+2^V N,1+2^V N}^C \end{pmatrix} \tag{5}$$

where

$$f_{i,j}^C = \begin{cases} f_{i,j}^\Pi, & \text{if } |f_{i,j}^\Pi| > \varepsilon \\ 0, & |f_{i,j}^\Pi| \le \varepsilon. \end{cases}$$

The reconstructed image of $f(x, y)$ is defined by

$$\tilde{F}^\Delta = (T'(N, V))^{-1} F^C T^{-1}(M, V). \tag{6}$$

The compression ratio is defined as the number of elements $f_{i,j}^C$, which is zero over the total number of elements $(1 + 2^V N)^2$. The average error and the maximum error between $\{\tilde{F}^\Delta\}$ and $\{F^\Delta\}$ are defined as follows:

$$\text{AverErr}\left(\tilde{F}^\Delta, F^\Delta\right) = \sqrt{\frac{\sum_i \sum_j \left(f(x_i, y_j) - \tilde{f}_{i,j}^\Delta\right)^2}{\sum_i \sum_j (f(x_i, y_j))^2}}$$

$$\text{MaxErr}\left(\tilde{F}^\Delta, f^\Delta\right) = \max \left| f(x_i, y_j) - \tilde{f}_{i,j}^\Delta \right|.$$

In summary, the conventional MoM impedance matrix generated by the usual triangular basis is transformed to a new matrix using the transformation of (1). Then the solution is obtained at a given scale. The solution is now extrapolated to the higher scale. If the computed second derivative of the solution is below a certain threshold at the new nodes, then the unknown of that node is discarded.

III. Implementation of AMMM in the Conventional Moment Method

Let S denote the surface of a square perfectly conducting plate in the xy plane. Let $\vec{E}^i$ be the electric field defined by an impressed source in the absence of the scatterer. The field is

incident on the structure and induces surface currents $\vec{J}$ on S. The induced current $\vec{J}$ can be written as

$$\vec{J}(\vec{r}) = J_x(\vec{r})\hat{x} + J_y(\vec{r})\hat{y} \tag{7}$$

where

$$J_x(\vec{r}) = \sum_{m=1}^{M} j_x^m \phi_x^m(\vec{r}), \quad J_y(\vec{r}) = \sum_{m=1}^{M} J_y^m \phi_y^m(\vec{r})$$

$\{\phi_x^m(\vec{r})\}$, $\{\phi_y^m(\vec{r})\}$ are the basis functions.

By the use of the Galerkin scheme and through the choice of $\{\phi_x^m(\vec{r})\}$, $\{\phi_y^m(\vec{r})\}$ as the tensor product of two triangular basis functions as the trial and the weighting function that are denoted by $\{\phi_i(\vec{r})\}$, the matrix equation will be equivalent to

$$\begin{pmatrix} A_{11} & A_{12} \\ A_{12} & A_{22} \end{pmatrix} \begin{pmatrix} \overline{J}_x \\ \overline{J}_y \end{pmatrix} = \frac{4\pi}{jk\eta_0} \begin{pmatrix} \overline{E}_x^i \\ \overline{E}_y^i \end{pmatrix} \tag{8}$$

where

$$\begin{aligned}
A_{11}(i,j) &= \int_S \phi_i(\vec{r})\,ds \int_S L_{11}(G\phi_j(\vec{r}'))\,ds', \\
A_{12}(i,j) &= \int_S \phi_i(\vec{r})\,ds \int_S L_{12}(G\phi_j(\vec{r}')\,ds' \\
A_{21}(i,j) &= \int_S \phi_i(\vec{r})\,ds \int_S L_{21}(G\phi_j(\vec{r}'))\,ds' \\
A_{22}(i,j) &= \int_S \phi_i(\vec{r})\,ds \int_S L_{22}(G\phi(\vec{r}'))\,ds' \\
L_{11} &= 1 + \frac{1}{k^2}\frac{\partial^2}{\partial x^2}, \quad L_{12} = \frac{1}{k^2}\frac{\partial^2}{\partial x \partial y}, \\
L_{22} &= 1 + \frac{1}{k^2}\frac{\partial^2}{\partial y^2} \\
G &= \frac{\exp\left[-jk\sqrt{(x-x')^2+(y-y')^2}\right]}{\sqrt{(x-x')^2+(y-y')^2}} \\
\vec{E}^i &= \left(E_\theta\hat{\theta} + E_\varphi\hat{\varphi}\right) \\
&\quad \cdot \exp[jk(x\sin\theta\cos\varphi + \sin\theta\sin\varphi)] \\
E_x^i &= \hat{x} \bullet \vec{E}^i, \quad E_y^i = \hat{y} \bullet \vec{E}^i \\
&\quad (i = 1, 2, \cdots, M \; j = 1, 2, \cdots, M) \\
\overline{J}_x &= (J_x^1, \cdots, J_x^M)^T, \quad \overline{J}_y = (J_y^1, \cdots, J_y^M)^T \\
\overline{E}_x^i &= (E_x^i(1), \cdots E_x^i(M))^T \\
\overline{E}_y^i &= (E_y^i(1), \cdots, E_y^i(M))^T \\
E_x^i(j) &= \int_s \phi_j(\vec{r}) E_x^i(\vec{r})\,ds \\
E_y^i(j) &= \int_s \phi_j(\vec{r}) E_y^i(\vec{r})\,ds.
\end{aligned}$$

The radar cross section (RCS) can be shown to have the following form:

$$\begin{aligned}
\sigma(\theta,\phi) &= \frac{k^2\eta_0^2}{4\pi} \\
&\cdot \left[\left|\sum_{n=1}^{M}(J_x^n\cos\theta\cos\phi + J_y^n\cos\theta\sin\phi)\zeta(\theta,\phi,n)\right|^2\right. \\
&\left. + \left|\sum_{n=1}^{M}(-J_x^n\sin\phi + J_y^n\cos\phi)\zeta(\theta,\phi,n)\right|^2\right] \\
&\cdot A^2(\theta,\phi)
\end{aligned} \tag{9}$$

TABLE I
RESULTS FOR A 1.1-λ SQUARE CYLINDER

Threshold	0.01	0.05	0.1
Reduced J_x	58	185	295
Reduced J_y	53	121	177
Actual size	771	576	410
Cond. No.	84787	185258	28693
CPU time(sec)	49.60	15.06	6.27

where $\zeta(\theta,\phi,n) = \exp[jk(x_n\sin\theta\cos\phi + y_n\sin\theta\sin\phi)]$

$$\begin{aligned}
A(\theta,\phi) &= T^2 \cdot \sin c^2\left[\frac{T\cdot k\cdot\sin\theta\cos\phi}{2}\right] \\
&\quad \cdot \sin c^2\left[\frac{T\cdot k\cdot\sin\theta\sin\phi}{2}\right].
\end{aligned}$$

Now we consider (8) using the multiscale basis functions. Suppose the 2-D triangular basis $\vec{\Phi}_\Delta(x,y)$ can be arranged as follows:

$$\vec{\Phi}(x,y) = \begin{pmatrix} \phi_1(y)\phi_1(x) \\ \vdots \\ \phi_1(y)\phi_{1+2^V N}(x) \\ \vdots \\ \vdots \\ \phi_{1+2^V N}(y)\phi_1(x) \\ \vdots \\ \phi_{1+2^V N}(y)\phi_{1+2^V N}(x) \end{pmatrix}$$

and the 2-D multiscale basis $\vec{\Psi}_\Pi^V(x,y)$ can be arranged as follows:

$$\begin{aligned}
&\vec{\Psi}_\Pi(x,y) \\
&\equiv \left(\vec{\psi}_0(y)\otimes\vec{\psi}_0(x),\ \vec{\psi}_0(y)\otimes\vec{\psi}_1(x),\ \vec{\psi}_1(y)\otimes\vec{\psi}_0(x),\right. \\
&\quad \vec{\psi}_1(y)\otimes\vec{\psi}_1(x),\ \vec{\psi}_0(y)\otimes\vec{\psi}_2(x),\ \vec{\psi}_2(y)\otimes\vec{\psi}_0(x) \\
&\quad \vec{\psi}_1(y)\otimes\vec{\psi}_2(x),\ \vec{\psi}_2(y)\otimes\vec{\psi}_1(x),\ \vec{\psi}_2(y)\otimes\vec{\psi}_2(x),\ \cdots \\
&\quad \vec{\psi}_0(y)\otimes\vec{\psi}_V(x),\ \vec{\psi}_V(y)\otimes\vec{\psi}_0(x),\ \vec{\psi}_1(y)\otimes\vec{\psi}_V(x) \\
&\quad \vec{\psi}_V(y)\otimes\vec{\psi}_1(x),\ \cdots,\ \vec{\psi}_V(y)\otimes\vec{\psi}_V(x) \\
&\quad \left.\vec{\psi}_V(y)\otimes\vec{\psi}_V(x)\right)^T
\end{aligned}$$

where $\vec{\psi}_v(x)$ and $\vec{\psi}_v(y)$ are the basis functions on vth scale along the x-axis and y-axis, respectively. Therefore, from zero-scale to three-scale, the number of the multiscale basis functions are $(1+N)^2$, $3N^2+2N$, $12N^2+4N$, $48N^2+8N$, respectively, at each of the four scales.

We can evaluate the transformation matrix $W(N,V)$ from the basis functions $\vec{\Phi}_\Delta(x,y)$ to the multiscale basis function in two dimension, $\vec{\Psi}_\Pi^V(x,y)$; that is

$$\vec{\Psi}_\Pi^V(x,y) = W(N,V)\vec{\Phi}_\Delta(x,y).$$

Therefore, (8) can be derived from the multiscale basis functions through

$$\begin{pmatrix} A_{11}^\Pi & A_{12}^\Pi \\ A_{21}^\Pi & A_{22}^\Pi \end{pmatrix} \begin{pmatrix} \overline{J}_x^\Pi \\ \overline{J}_y^\Pi \end{pmatrix} = \frac{4\pi}{jk\eta_0} \begin{pmatrix} \overline{E}_x^{i\Pi} \\ \overline{E}_y^{i\Pi} \end{pmatrix} \tag{8'}$$

where $\overline{E}^{i\Pi}_{x,y} = W(N, V)\overline{E}^{i}_{x,y}$, $\overline{J}_{x,y} = W^T(N, V)\overline{J}^{\Pi}_{x,y}$, $A^{\Pi}_{x,y} = W(N, V)A_{i,j}W^T(N, V)$. The coefficient matrices $A^{\Pi}_{i,j}(A^{\Pi}_{i,j}(0), \cdots, A^{\Pi}_{i,j}(V))$ the unknowns $\overline{J}^{\Pi}_{x,y}(\overline{J}^{\Pi}_{x,y}(0)\cdots, \overline{J}^{\Pi}_{x,y}(V))$ and the array $\overline{E}^{i\Pi}_{x,y}(\overline{E}^{i\Pi}_{x,y}(0), \cdots, \overline{E}^{i\Pi}_{x,y}(V))$ are arranged in the scaled-block form (see Fig. 2).

The scheme of the adaptive multiscale moment method to solve the matrix equations (8′) from the (v)th scale to the $(v+1)$th scale is given as follows.

Step 1) Suppose the solutions $(\overline{J}^{\Pi}_{x,y}(0), \cdots, \overline{J}^{\Pi}_{x,y}(v))$ on the (v)th scale are given. Then the actual solution $\{\overline{J}_{x,y}(v)\}$ on the coarse grid can be obtained by the use of the following formula:

$$\overline{J}_{x,y}(v) = W^T(N, v)\begin{pmatrix} \overline{J}^{\Pi}_{x,y}(0) \\ \overline{J}^{\Pi}_{x,y}(1) \\ \overline{J}^{\Pi}_{x,y}(v) \end{pmatrix}.$$

Step 2) Estimate the solution $\{\overline{J}_{x,y}(v+1)\}$ on the finer grid through the use of a 2-D interpolant formula such as a tensor product spline interpolant [35]. The tensor product spline interpolant function to the data $\{f(x_i, y_i)\}$, where $\{1 \le i \le N_x\}$ and $\{1 \le j \le N_y\}$, has the form

$$\sum_{m=1}^{N_y}\sum_{n=1}^{N_x} c_{nm}B_{n,k_x,t_x}(x)B_{m,k_y,t_y}(y)$$

where $B_{i,k,t}(s)$ is vth (normalized) B-spline of order k for the knot sequence t. The coefficients $c_{n,m}$ can be computed from the following solution of the system of equations:

$$\sum_{m=1}^{N_y}\sum_{n=1}^{N_x} c_{nm}B_{n,k_x,t_x}(x_i)B_{m,k_y,t_y}(y_j) = f(x_i, y_j)$$
$$\{1 \le i \le N_x,\ 1 \le j \le N_y\}.$$

Step 3) Get the initial guess on the finer grid using the following formula:

$$\begin{pmatrix} \overline{J}^{\Pi}_{x,y}(0) \\ \overline{J}^{\Pi}_{x,y}(1) \\ \vdots \\ \overline{J}^{\Pi}_{x,y}(v+1) \end{pmatrix} = (W^T(N, v+1))^{-1}\overline{J}_{x,y}(v+1).$$

Step 4) If the elements of $\{\overline{J}^{\Pi}_{x,y}(k)\}$ $(k = 1, 2, 3, \cdots, v+1)$ are less than ε (the given threshold parameter), we set these elements to zero and delete the corresponding rows and columns of the coefficient matrices $A^{\Pi}_{i,j}$ and the corresponding elements of the array $\overline{E}^{i\Pi}_{x,y}$ on the $(v+1)$th scale. Then after reducing the size of the original linear equation, the modified linear equation and the initial guess are obtained.

Step 5) Solve the modified linear equation by use of the iterative method or LU method. Adding these elements which are set to be zero in Step 4), the solution $\{\overline{J}^{\Pi}_{x,y}(0), \cdots, \overline{J}^{\Pi}_{x,y}(v), \overline{J}^{\Pi}_{x,y}(v+1)\}$ on the multiscale triangular basis are obtained. Using the step one, we can obtain the original solutions on the finer grid.

This procedure continues until the largest scale is reached. Typically, it has been our experience that it is not necessary to go beyond the third scale.

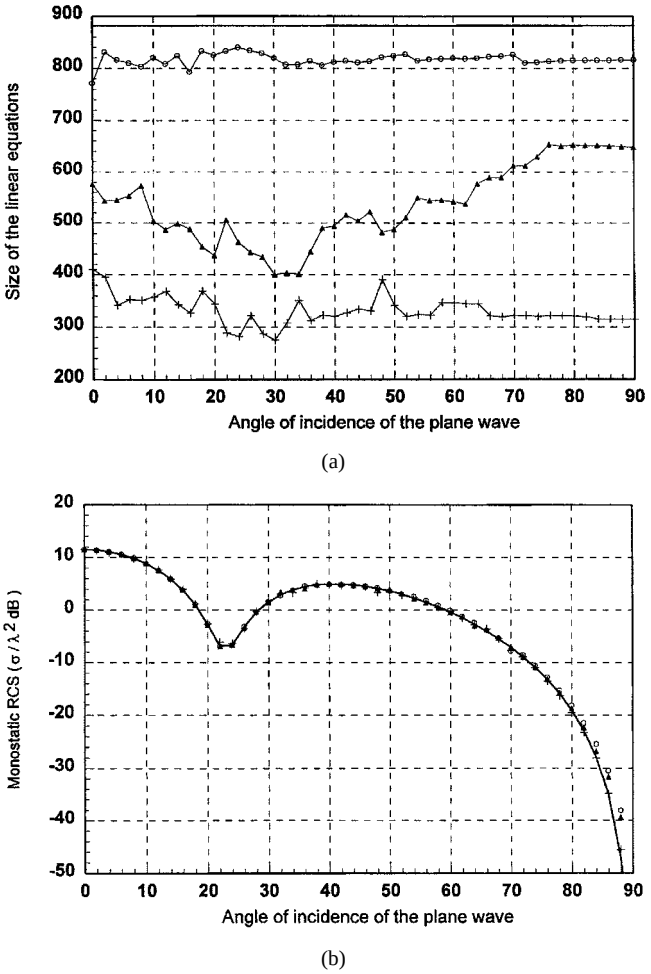

Fig. 4. (a) The actual size of the linear equations versus the angle of incidence. (b) The monostatic RCS versus the angle of incidence. The circle, triangle, and cross signals denote the results for the threshold $\varepsilon = 0.01,\ 0.05,\ 0.1$. The solid line presents the result of the conventional moment method. The monostatic and the size of the linear equations for V-polarized plane wave.

IV. Numerical Results

In this section, we discuss some numerical examples for analyzing scattering from perfectly conducting plates by the 2-D AMMM. All of the numerical simulations have been performed on DELL OptiPlex Gxi 166 MHz 512 RAM personal computer in a multitasking environment.

First, consider the scattering from a $1.1\lambda \times 1.1\lambda$ perfectly conducting plate. The plate is discretized into $2l \times 2l$ cell; that is, the center of the cells is (iT, jT) $(T = 0.05\lambda, i, j = 0, \pm1, \pm2, \cdots, \pm10)$. The basis and weighting functions are chosen by $\{\phi(x - iT)\phi(y - jT)\}$, where

$$\phi(t) = \begin{cases} 1 - |t|/T, & |t| \le T \\ 0, & \text{otherwise.} \end{cases}$$

Total number of nodes is 441 and the total number of unknowns for the linear equations is 882. The largest scale is taken as two. So the total number of unknowns for J_x, and J_y is $(5 \cdot 2^0 + 1)^2$, $(5 \cdot 2^1 + 1)^2$, $(5 \cdot 2^2 + 1)^2$ from zero scale to two scale, respectively.

For the different thresholds, the reduced number of J_x and J_y, the actual size of the linear equations, and the condition number on the two scale are given in Table Iwhen the conducting plate is illuminated by an incident plane wave with the magnetic field vector oriented along the $+y$ axis.

The condition numbers of the original coefficient matrix and the coefficient matrix on the 2-D multiscale basis are 1888 and 50 532, respectively. The CPU time required for just the solution of the conventional moment method is 64.32(s). The bistatic RCS is shown in Fig. 3.

In Table I, CPU time is the time required to solve the linear equations by use of the conventional moment method or the adaptive multiscale moment method. This does not include the time spent to compute the original impedance matrix, which is common in all the procedures.

From Table I, it is seen that the smaller the threshold, fewer unknowns have been eliminated. There is no relationship between the condition number and the actual size of the modified linear equation. This is a problem with a wavelet-type methodology. When the threshold is taken as 0.01, 0.05, 0.1, the size of the linear equation is reduced by about 13%, 35%, and 54%, respectively, and the errors of the bistatic RCS are very small (see Fig. 4).

For the different thresholds, the monostatic RCS and the actual size of the linear equations on the two scale versus the angle of incidence with E-polarized plane wave are plotted in Fig. 5.

Consider the solution of electromagnetic scattering from a $2.1\lambda \times 2.1\lambda$ perfectly conducting plate. The total number of unknowns in the conventional method of moment for J_x and J_y are 1681. The total number of unknowns for the linear equations are 3362. The largest scale can be taken as two. So the number of unknowns for J_x and J_y are $(10 \cdot 2^0 + 1)^2$ at the zeroth scale, $(10 \cdot 2^1 + 1)^2$ at first scale and $(10 \cdot 2^2 + 1)^2$ at second scale, respectively. Also, when the number of unknowns exceeds a few thousand unknowns, the matrix solution time generally exceeds the matrix fill time. The matrix fill time in this case is 392(s). The matrix solution time utilizing the conventional moment method is 3934.31(s).

For the different thresholds, the reduced number of J_x and J_y, the actual size of the linear equations, and the condition number on the two scale are given in Table II, when the conducting plate is illuminated by an incident plane wave with the magnetic field vector oriented along the $+y$ axis.

The CPU time is the time required to solve only the linear equation by use of the conventional moment method or the adaptive multiscale moment method. This does not include the time spent to compute the original MoM impedance matrix.

The condition numbers of the original coefficient matrix and the coefficient matrix on the 2-D multiscale basis are 1435 and 23 110, respectively. The bistatic RCS are shown in Fig. 5. It is interesting to note that for $\varepsilon = 0.05$, there is an improvement in the condition number (7240 as opposed to 23 110).

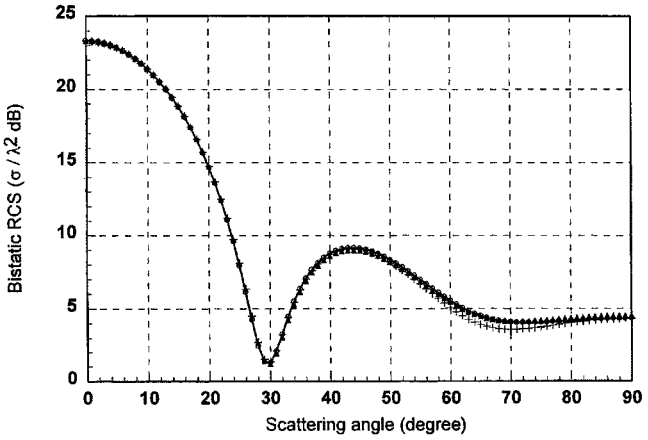

Fig. 5. The bistatic RCS of a 2.1 square plates by a normally incident plane wave versus the scattering angle on $\phi = 0°$ plane. The circle, triangle, and cross signals denote the results for the threshold $\varepsilon = 0.01,\ 0.05,\ 0.1$. The solid line denotes the result of the conventional moment method.

TABLE II
RESULTS FOR THE 2.1-λ SQUARE CYLINDER

Threshold	0.01	0.05	0.1
Reduced J_x	717	1151	1262
Reduced J_y	585	1074	1204
Actual size	2060	1137	896
Cond. No.	360164	7240	9780
CPU time(sec)	901.34	218.28	158.04

For the different thresholds, the monostatic RCS and the actual size of the linear equation on the two scale versus the angle of incidence with E-polarized plane wave are plotted in Fig. 6.

V. CONCLUSIONS

Two-dimensional AMMM has been used to analyze scattering from perfectly conducting plates. By use of the matrix transformation, the impedance matrix and the source terms constructed by the conventional moment method can be transformed by a matrix into the form of basis functions being applied at different scales. The initial guess for the unknown $\overline{J}^{\,\mathrm{II}}_{x,\,y}$, in the multiscale basis on the finer scale can be obtained from the initial guess of the functions $J_x(\vec{r})$, $J_y(\vec{r})$ on the finer scale which are predicted from the previous scale by the multigrid method.

Two examples have been presented to illustrate that AMMM can reduce automatically the size of the linear equations and can improve the efficiency of the conventional moment method.

Although the matrix transformation in the 2-D AMMM is derived from the tensor product of two triangular basis functions over a uniform grid, the 2-D AMMM has no restriction for adaptation to any kind of basis function in the moment method. Furthermore, the analysis can be extended in a straightforward manner to solve scattering or radiation problems dealing with complicated objects.

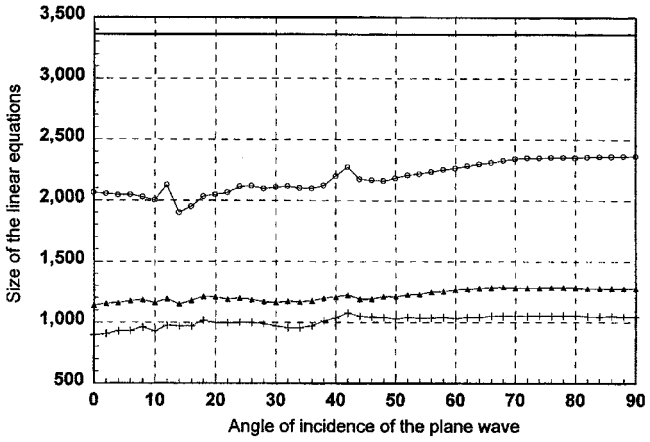

(a)

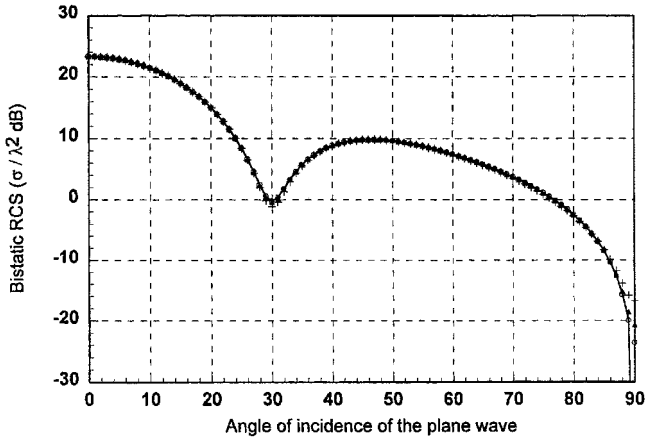

(b)

Fig. 6. The bistatic RCS versus the scattering angle on $\phi = 0°$ plane. (b) The bistatic RCS versus the scattering angle on $\phi = 90°$ plane. The circle, triangle, and cross signals denote the results for the threshold $\varepsilon = 0.01,\ 0.05,\ 0.1$. The solid line denotes the result of the conventional moment method. The bistatic RCS of a 2.1 square plates by a normally incident plane wave with the magnetic field vector oriented along the $+y$ axis.

REFERENCES

[1] R. F. Harrington, *Field Computation by Moment Method*. New York: MacMillan, 1968.

[2] E. K. Miller, L. Medgyesi-Mitschang, and E. H. Newman, Eds., *Computational Electromagnetics: Frequency-Domain Method of Moments*. New York: IEEE Press, 1992.

[3] D. P. Bouche, F. A. Molinet, and R. Mittra, "Asymptotic and hybrid techniques for electromagnetic scattering," *Proc. IEEE*, vol. 81, pp. 658–1684, Dec. 1993.

[4] G. A. Thiele, "Overview of selected hybrid method in radiating system analysis," *Proc. IEEE*, vol. 80, pp. 67–78, Jan. 1992.

[5] L. N. Medgyesi-Mitschang and D. S. Wang, "Hybrid methods in computational electromagnetics: A review," *Comput. Phys. Commun.*, vol. 68, pp. 76–94, May 1991.

[6] F. X. Canning, "The impedance matrix localization method (IML) uses," *IEEE Trans. Antennas Propagat.*, vol. 41, pp. 659–667, May 1993.

[7] ——, "The impedance matrix localization method (IML) permits solution of large scatterers," *IEEE Magn.*, vol. 27, pp. 4275–4277, Sept. 1991.

[8] ——, "The impedance matrix localization method (IML) for MM calculation," *IEEE Trans. Antennas Propagat.*, vol. 32, pp. 18–30, Oct 1990.

[9] ——, "Transformations that produce a sparse moment method matrix," *J. Electromagn. Wave Applicat.*, vol. 4, no. 9, pp. 893–913, 1990.

[10] R. Coifman, V. Rohklin, and S. Wandzura, "The fast multipole method for the wave equation: A pedestrian prescription," *IEEE Antennas Propagat. Mag.*, vol. 35, pp. 7–12, 1993.

[11] V. Rohklin, "Rapid solution of integral equations of scattering in two dimensions," *J. Comput. Phys.*, vol. 86, pp. 414–439, 1990.

[12] ——, "Rapid solution of integral equations of classical potential theory," *J. Comput. Phys.*, vol. 60, pp. 187–207, 1985.

[13] A. Boag and R. Mittra, "Complex multipole beam approach to electromagnetic scattering problems," *IEEE Trans. Antennas Propagat.*, vol. 42, pp. 366–372, Mar. 1994.

[14] E. Michielssen and A. Boag, "Multilevel evaluation of electromagnetic fields for the rapid solution of scattering problems," *Microwave Opt. Tech. Lett.*, vol. 7, no. 17, pp. 790–795, Dec. 1994.

[15] ——, "A multilevel matrix decomposition algorithm for analyzing scattering from large structures," in *11th Annu. Rev. Progress ACES*, Monterey, CA, Mar. 1995, pp. 614–620.

[16] ——, "A multilevel matrix decomposition algorithm for analyzing scattering from large structures," *IEEE Trans. Antennas Propagat.*, vol. 44, pp. 1086–1093, Aug. 1996.

[17] G. Beylkin, R. Coifman, and V. Rokhlin, "Fast wavelet transform and numerical algorithm I," *Comm. Pure Appl. Math.*, vol. 44, pp. 141–183, 1991.

[18] B. K. Alpert, G. Beylkin, R. Coifman, and V. Rokhlin, "Wavelet-like bases for the fast solution of second-kind integral equation," *SIAM J. Sci. Comp.*, vol. 14, pp. 159–184, Jan. 1993.

[19] B. Z. Steinberg and Y. Leviatan, "On the use of wavelet expansions in the method of moments," *IEEE Trans. Antennas Propagat.*, vol. 41, pp. 610–619, 1993.

[20] J. C. Goswami, A. K. Chan, and C. K. Chui, "On solving first-kind integral equations using wavelets on a bounded interval," *IEEE Trans. Antennas Propagat.*, vol. 43, pp. 614–622, June 1995.

[21] G. F. Wang, "A hybrid wavelet expansion and boundary element analysis of electromagnetic scattering from conducting objects," *IEEE Trans. Antennas Propagat.*, vol. 42, pp. 170–178, Feb. 1995.

[22] W. C. Chew, J. M. Jin, C. C. Lu, E. Michielssen, and J. M. Song, "Fast solution methods in electromagnetics," *IEEE Trans. Antennas Propagat.*, vol. 45, pp. 533–543, Mar. 1997.

[23] C. Su and T. K. Sarkar, "A multiscale moment method for solving Fredholm integral equation of the first kind," *J. Electromagn. Waves Appl.*, vol. 12, pp. 97–101, 1998.

[24] ——, "Scattering from perfectly conducting strips by utilizing an adaptive multiscale moment method," *Progress Electromagn. Res.*, vol. PIER 19, pp. 173–197, 1998.

[25] ——, "Electromagnetic scattering from coated strips utilizing the adaptive multiscale moment method," *Progress Electromagn. Res.*, vol. PIER 18, pp. 173–208, 1998.

[26] ——, "Electromagnetic scattering from two-dimensional electrically large perfectly conducting objects with small cavities and humps by use of adaptive multiscale moment methods (AMMM)," *J. Electromagn. Waves Appl.*, vol. 12, pp. 885–906, 1998.

[27] ——, "Adaptive multiscale moment method for solving two-dimensional Fredholm integral equation of the first kind," *J. Electromagn. Waves Appl.*, vol. 13, no. 2, pp. 175–176, 1999.

[28] A. Brandt, "Multi-level adaptive solutions to boundary value problems," *Math. Comput.*, vol. 31, pp. 330–390, 1977.

[29] W. Hackbusch, *Multigrid Methods and Applications*. New York: Springer-Verlag, 1985.

[30] S. F. McCormick, *Multigrid Methods: Theory, Application, and Supercomputing*. New York: Marcel Dekker, 1988.

[31] J. Mandel, "On multilevel iterative methods for integral equations of the second kind and related problems," *Numer. Math.*, vol. 46, pp. 147–157, 1985.

[32] P. W. Hemker and H. Schippers, "Multiple grid methods for the solution of Fredholm integral equations of the second kind," *Math. Comput.*, vol. 36, no. 153, 1981.

[33] K. Kalbasi and K. R. Demarest, "A multilevel enhancement of the method of moments," in *7th Annu. Rev. Progress Appl. Computat. Electromagn.*. Monterey, CA, Mar. 1991, pp. 254–263.

[34] ——, "A multilevel formulation of the method of moments," *IEEE Trans. Antennas Propagat.*, vol. 41, pp. 589–599, May 1993.

[35] de Boor, *A Practical Guide to Splines*. New York: Springer-Verlag, 1978.

[36] T. K. Sarkar and K. Kim, "Solution of large dense complex matrix equations utilizing wavelet-like transforms," *IEEE Trans. Antennas Propagat.*, vol. 47, pp. 1628–1632, Oct. 1999.

Chaowei Su, photograph and biography not available at time of publication.

T. K. Sarkar (S'69–M'76–SM'81–F'92) received the B.Tech. degree from the Indian Institute of Technology, Kharagpur, India, in 1969, the M.Sc.E. degree from the University of New Brunswick, Fredericton, Canada, in 1971, and the M.S. and Ph.D. degrees from Syracuse University, Syracuse, NY, in 1975.

From 1975 to 1976, he was with the TACO Division of the General Instruments Corporation. He was with the Rochester Institute of Technology, Rochester, NY, from 1976 to 1985. He was a Research Fellow at the Gordon McKay Laboratory, Harvard University, Cambridge, MA, from 1977 to 1978. He is now a Professor in the Department of Electrical and Computer Engineering, Syracuse University. He was an associate editor for feature articles of the *IEEE Antennas and Propagation Society Newsletter* and has authored or coauthored more than 210 journal articles and numerous conference papers. He has written chapters in 28 books and ten books, including *Iterative and Self-Adaptive Finite-Elements in Electromagnetic Modeling* (Norwood, MA: Artech House, 1998). His current research interests deal with numerical solutions of operator equations arising in electromagnetics and signal processing with application to system design.

Dr. Sarkar received one of the "Best Solution" Awards in May 1977 at the Rome Air Development Center (RADC) Spectral Esitmation Workshop. He is a registered Professional Engineer in New York State. He received the Best Paper Award of the IEEE TRANSACTIONS ON ELECTROMAGNETIC COMPATIBILITY in 1979 and at the 1997 National Radar Conference. He received the College of Engineering Research Award in 1996 and the Chancellor's Citation for Excellence in Research in 1998 at Syracuse University. He was the Technical Program Chairman for the 1998 IEEE Antennas and Propagation Society International Symposium and URSI on Time Domain Metrology (1990–1996). He is a member of Signa Xi and the International Union of Radio Science Commissions A and B. He received the title *Docteur Honoris Causa* from Universite Blaise Pascal, Clermont Ferrand, France, in 1998.